NuSmear: Fast Simulation of Energy Smearing and Angular Smearing in Neutrino Scattering Events

Via Generic Parameterized Models in the GENIE Event Generator

Ishaan Vohra
Phillips Exeter Academy, New Hampshire
CIPANP 2022

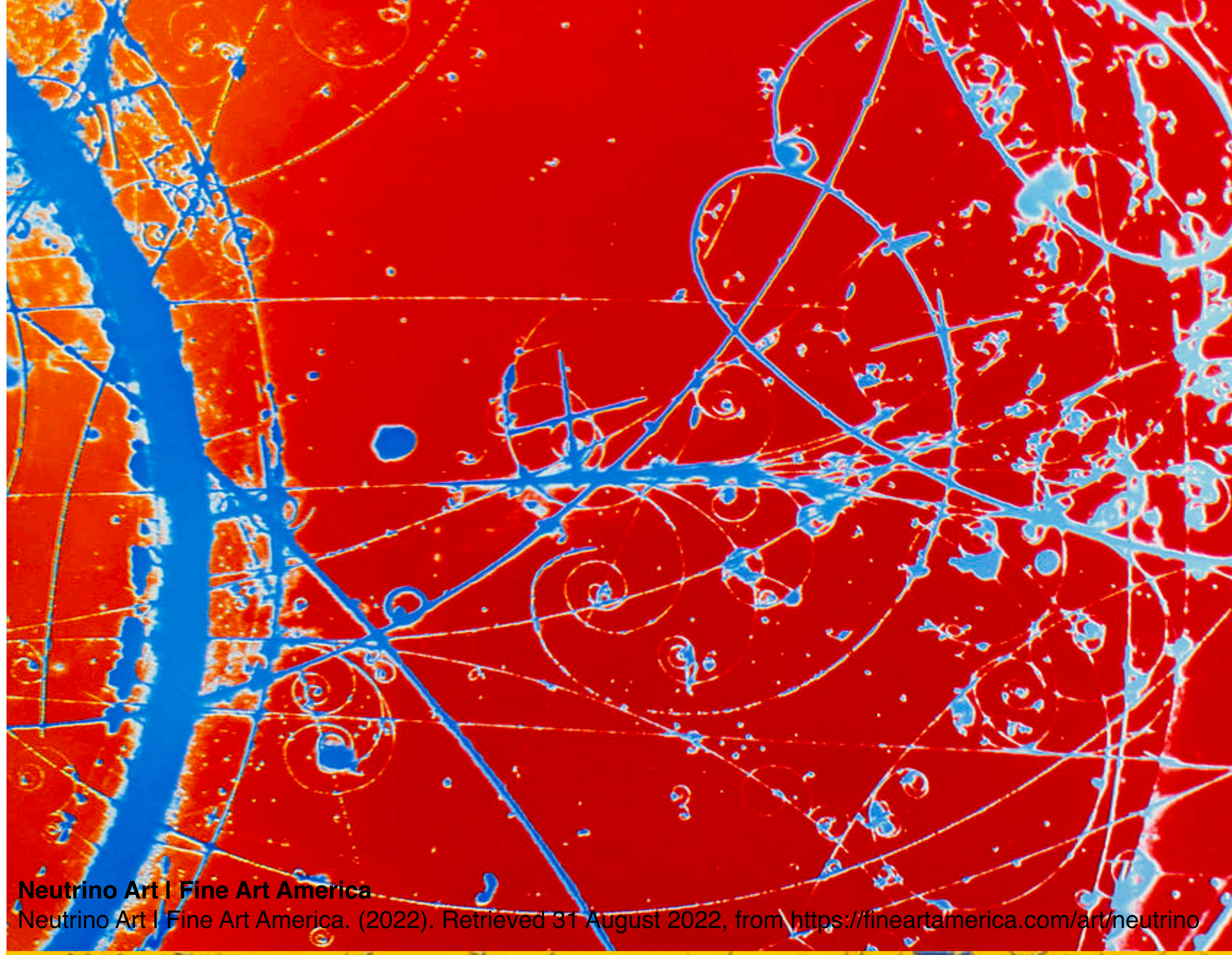

Neutrino Art | Fine Art America
Neutrino Art | Fine Art America. (2022). Retrieved 31 August 2022, from https://fineartamerica.com/art/neutrino

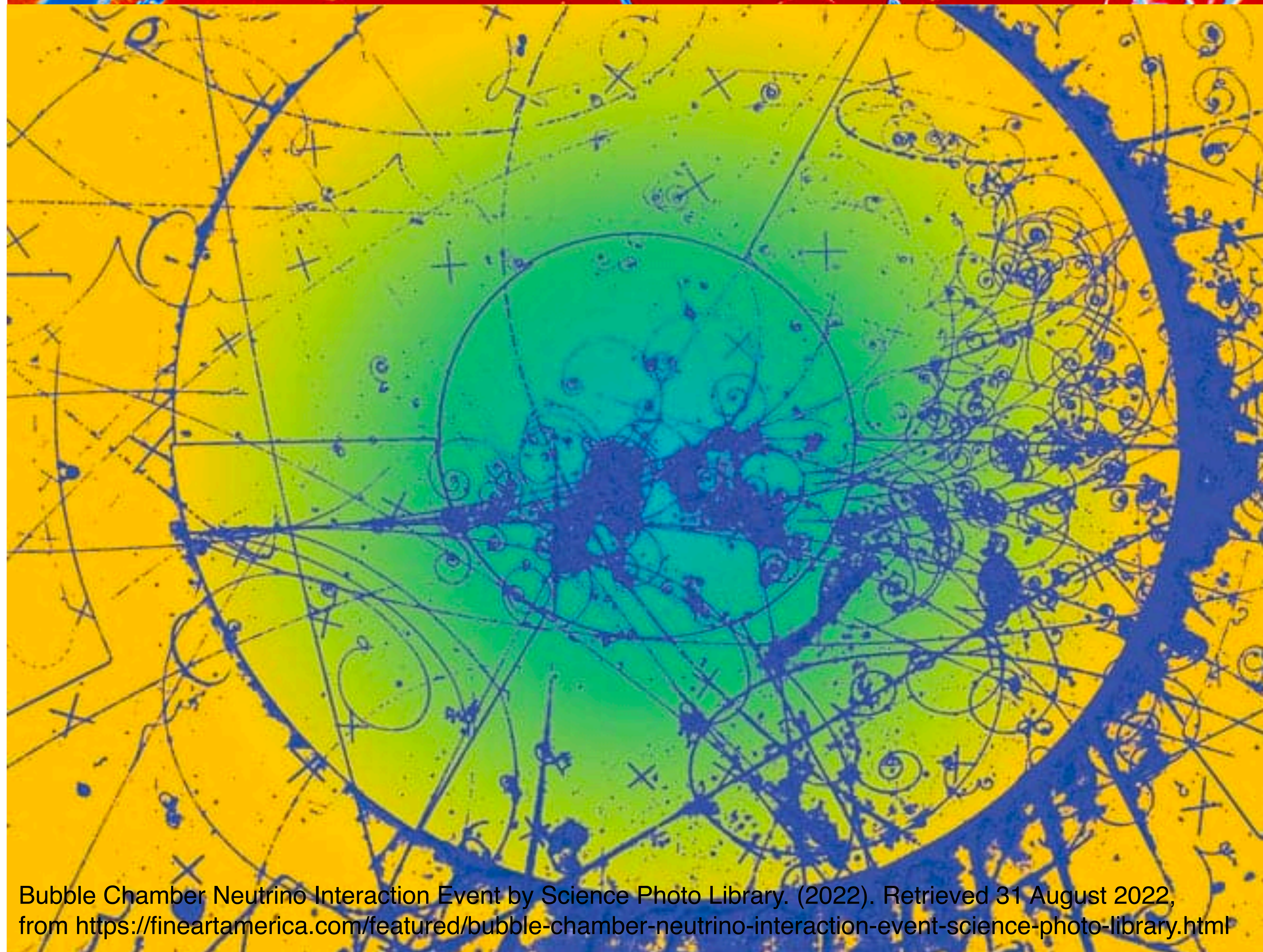

Bubble Chamber Neutrino Interaction Event by Science Photo Library. (2022). Retrieved 31 August 2022, from https://fineartamerica.com/featured/bubble-chamber-neutrino-interaction-event-science-photo-library.html

Overview

- Introduction
  - Motivation
  - What Is NuSmear?
- Simulation methodology
  - Computation of smearing resolution
  - Smearing distributions
  - Particle detection dependency
- Validation of smearing performance
  - Energy smearing operation
  - Angular smearing operation

Introduction

Motivation

- The ability of Monte Carlo (MC) methods to provide detailed simulations for neutrino events plays an essential role in both data analysis and the planning of future experiments, however complete simulations are often lengthy and CPU-intensive.

For preliminary simulations, the solution is fast Monte Carlo methods.

- Balancing between physical accuracy of simulations and speed of computation.

Motivation

Within the area of detector response simulations:

- DELPHES
- EIC Smear
- ATLAS Fast Track Simulation Project

But within the neutrino physics community,

- Tools for specific experimental setups (e.g. GLoBES)
- Few systems providing rapid preliminary smearing simulations for generic neutrino-nucleon scattering events

DELPHES fast simulation

eic/eic-smear

What Is NuSmear?

- Energy smearing and angular smearing via parameterized model-based presets.
- Fast, generic, geometry-independent.
- Contribution package built onto the GENIE Monte Carlo event generator.
- Simulates energy and angular smearing between all flavors of neutrinos and nuclear targets within the MeV to PeV energy scales.

NuSmear

Simulation Process

1. Smearing model selection
2. Computation of resolution
3. Application of smearing distribution
4. Consideration of detection dependency

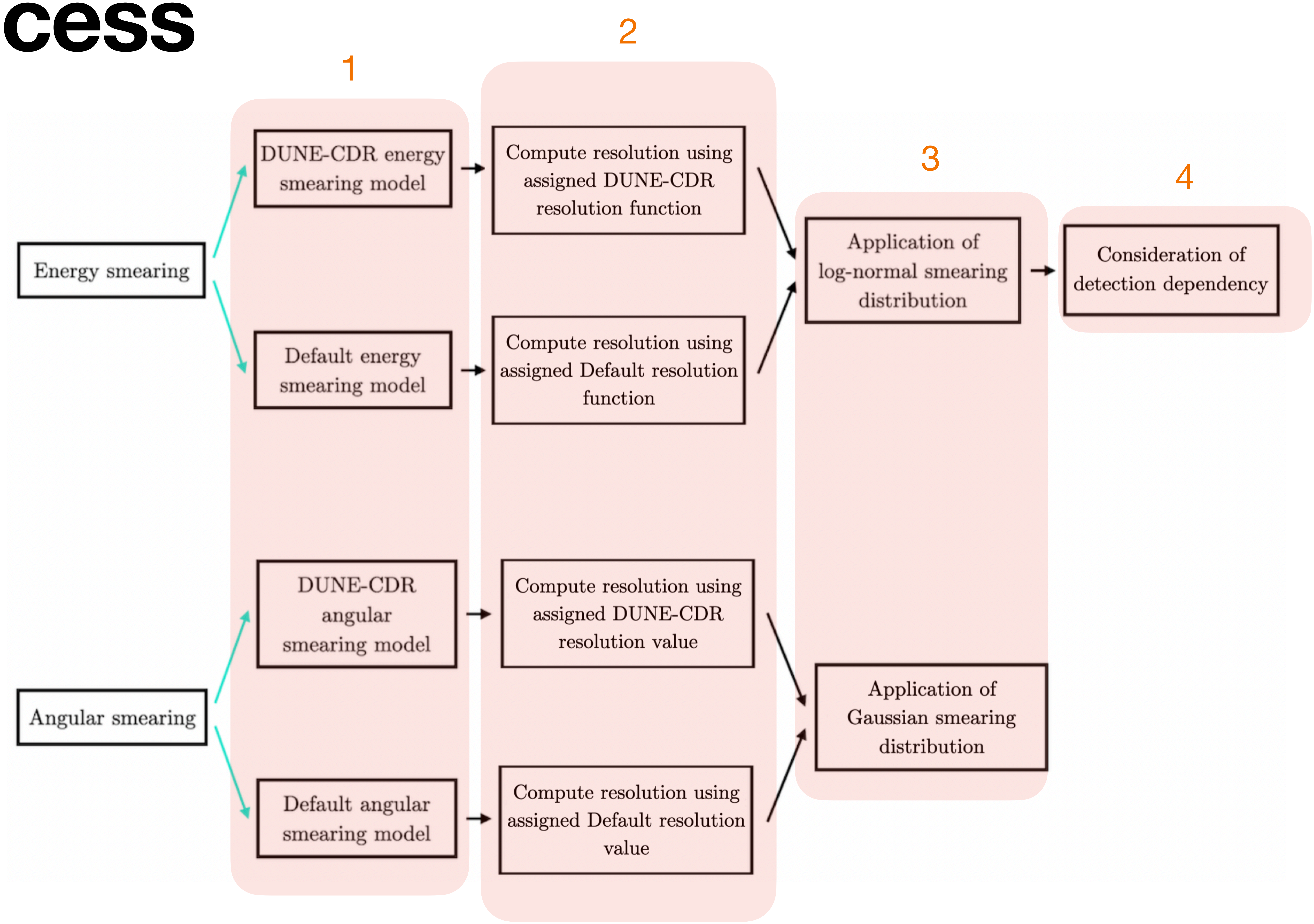

Simulation Methodology

Energy Resolution Computation - DUNE-CDR Model

- Up to three particle parameters to compute an energy resolution: total energy, kinetic energy, and magnitude of momentum.
- If a particle doesn't pass the KE threshold, returns zero reconstructed energy.
- All DUNE-CDR geometric dependencies are omitted and approximated using numerical values.

Particle type	Function calculations	Omitted dependencies
$\pi^{\pm}$	if KE $\geq$ 100 MeV, return 15%	track length, showering, contained/exiting track
γ, $e^{\pm}$	if KE $\geq$ 30 MeV, return $2\% \oplus 15\%/\sqrt{E}$[GeV]	
$p/\bar{p}$	if KE $\geq$ 50 MeV, return 10% if $\lvert$p$\rvert$ < 400 MeV/c, else return $5\% \oplus 30\%/\sqrt{E}$[GeV]	
$\mu^{\pm}$	if KE $\geq$ 30 MeV, return 15%	track length, contained/exiting track
$n/\bar{n}$	if KE $\geq$ 50 MeV, return $40\%/\sqrt{E}$[GeV]	
other	if KE $\geq$ 50 MeV, return $5\% \oplus 5\%/\sqrt{E}$[GeV]	

Table 1: Summary of the calculations performed by NuSmear's energy resolution functions in the DUNE-CDR model. E, KE, and $\lvert$p$\rvert$ denote total energy, kinetic energy, and magnitude of momentum respectively.

Energy Resolution Computation - Default Model

- Simpler calculations than that of the DUNE-CDR model.
- Single threshold comparison: check if KE > 50 MeV.

Particle type	Energy resolution
$\pi^{\pm}$,π^0	15%
$K^{\pm}$, $K^0/\bar{K}^0$	20%
γ	30%
$e^{\pm}$	40%
$p/\bar{p}$	40%
$\mu^{\pm}$	15%
$n/\bar{n}$	50%
other	30%

Table 2: Summary of the energy resolution values assigned to each particle type in the Default model.

Angular Resolution Computation - DUNE-CDR and Default Models

- Angular resolution value determined purely by particle type.
- On average *more conservative* than the DUNE-CDR model

Particle type	Angular resolution	
	DUNE-CDR model	Default model
$\pi^{\pm}$	1°	2°
π^{0}	5°	8°
$K^{\pm}$	5°	2°
$K^{0}/\bar{K}^{0}$	5°	8°
γ, $e^{\pm}$	1°	3°
$p/\bar{p}$	5°	8°
$\mu^{\pm}$	1°	2°
$n/\bar{n}$	5°	10°
other	5°	8°

Table 3: Summary of the angular resolution values assigned to each particle type in the DUNE-CDR and Default models.

Smearing Distributions - Energy Smearing

- Commonly used Gaussian distribution - how to exclude negative energy?
- Truncation reduces the simulation's accuracy to a real detector at low energies.
- NuSmear uses the log-normal distribution instead.

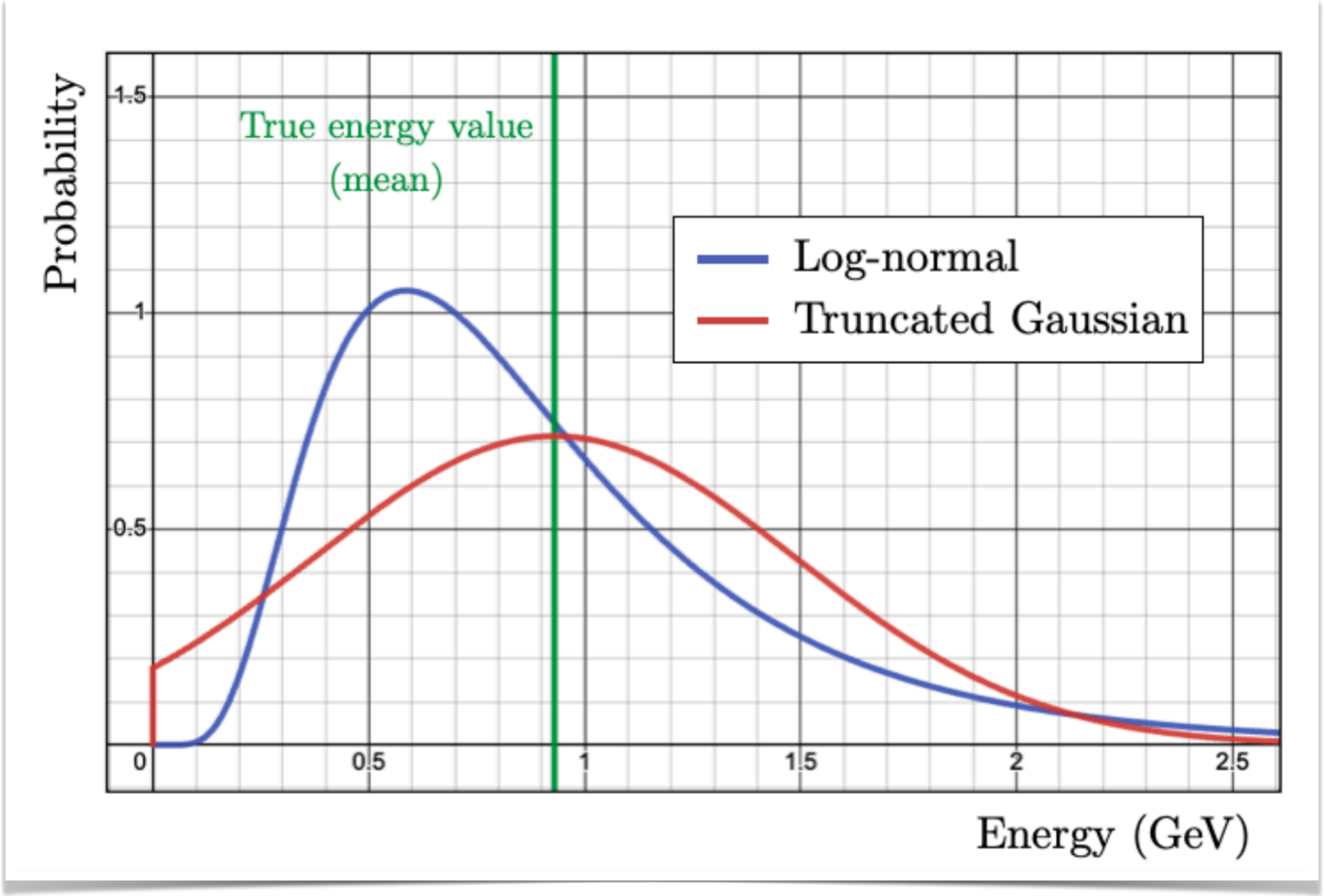

Smearing Distributions - Energy Smearing

- Log-normal distribution takes the form

$$f(x) = \frac{1}{x\sigma\sqrt{2\pi}} \exp\left(-\frac{(\ln(x)-\mu)^2}{2\sigma^2}\right)$$

- Parameters μ and σ are given in terms of m and $Var[X]$

$$\mu = \ln\left(\frac{m^2}{\sqrt{Var[X]+m^2}}\right),$$

$$\sigma^2 = \ln\left(1 + \frac{Var[X]}{m^2}\right).$$

- Moreover, m and $Var[X]$ are related to E_{true} and R_E by

$$m = E_{true},$$

$$Var[X] = (R_E E_{true})^2.$$

Mersenne Twister pseudo-random number generator (PRNG) to generate reconstructed energy.

Smearing Distributions - Angular Smearing

- Particle's outgoing angle with respect to the incident neutrino, θ.
- Gaussian distribution:
  - $\mu = \theta$
  - $\sigma = R_A$
- Mersenne Twister generates reconstructed angle.

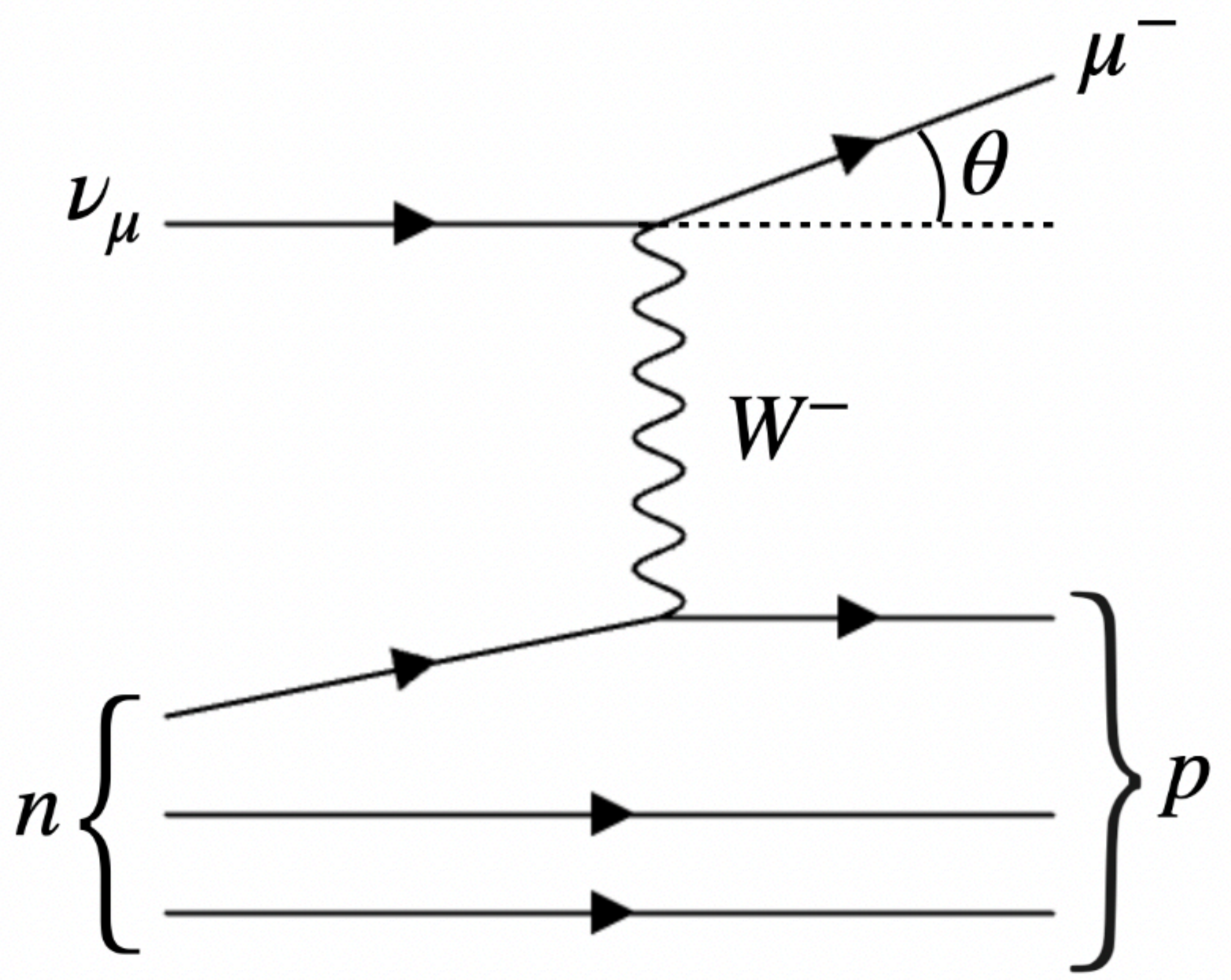

Figure 3: Example charged-current (CC) interaction between an incident muon neutrino and neutron, producing an outgoing muon at angle θ with respect to the incident neutrino.

Smearing Distributions - Angular Smearing

- Particle's outgoing angle with respect to the incident neutrino, θ.
- Gaussian distribution:
  - $\mu = \theta$
  - $\sigma = R_A$
- Mersenne Twister generates reconstructed angle.

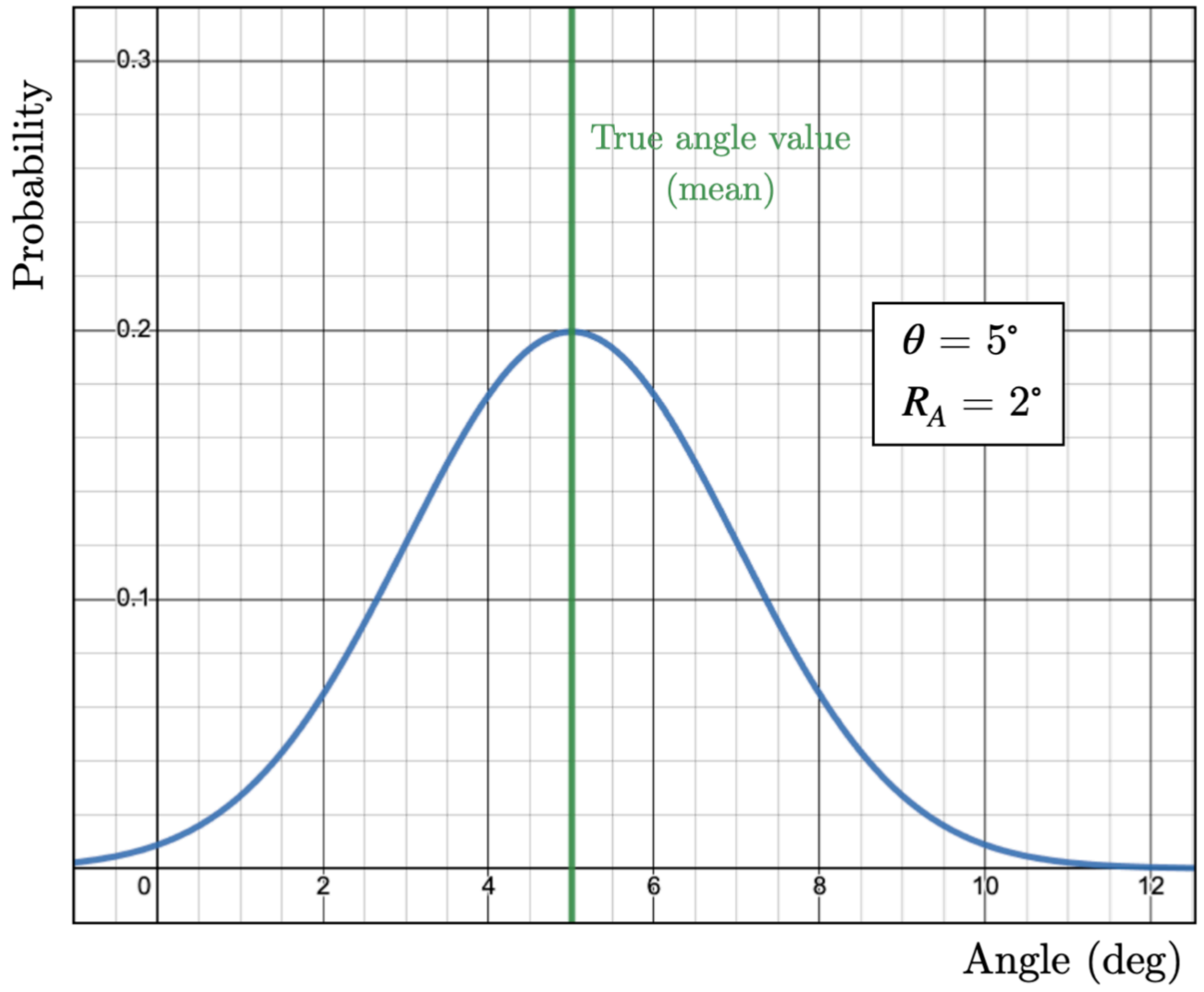

Figure 4: Example Gaussian smearing distribution with a true angle value of 5° and an angular resolution of 2°.

Particle Detection Dependency

- More accurately simulate unobserved particles in real detectors.
- Within NuSmear's DUNE-CDR model:
  - Neutrons: $|p| < 1$ GeV/c $\rightarrow$10% probability of escaping detection.
  - (Detected) neutrons: 60% of the energy generated by the smearing distribution is returned to the user.
- Within NuSmear's Default model:
  - Photons, neutrons, and antineutrons $\rightarrow$ 50% probability of escaping detection.

Validation of Smearing Performance

Energy Smearing - Complete MC Comparison

- Incoming electron neutrino flux derived from the the OPERA neutrino experiment.
- Compare neutrino energy smearing matrices (CC only) with OPERA complete MC.

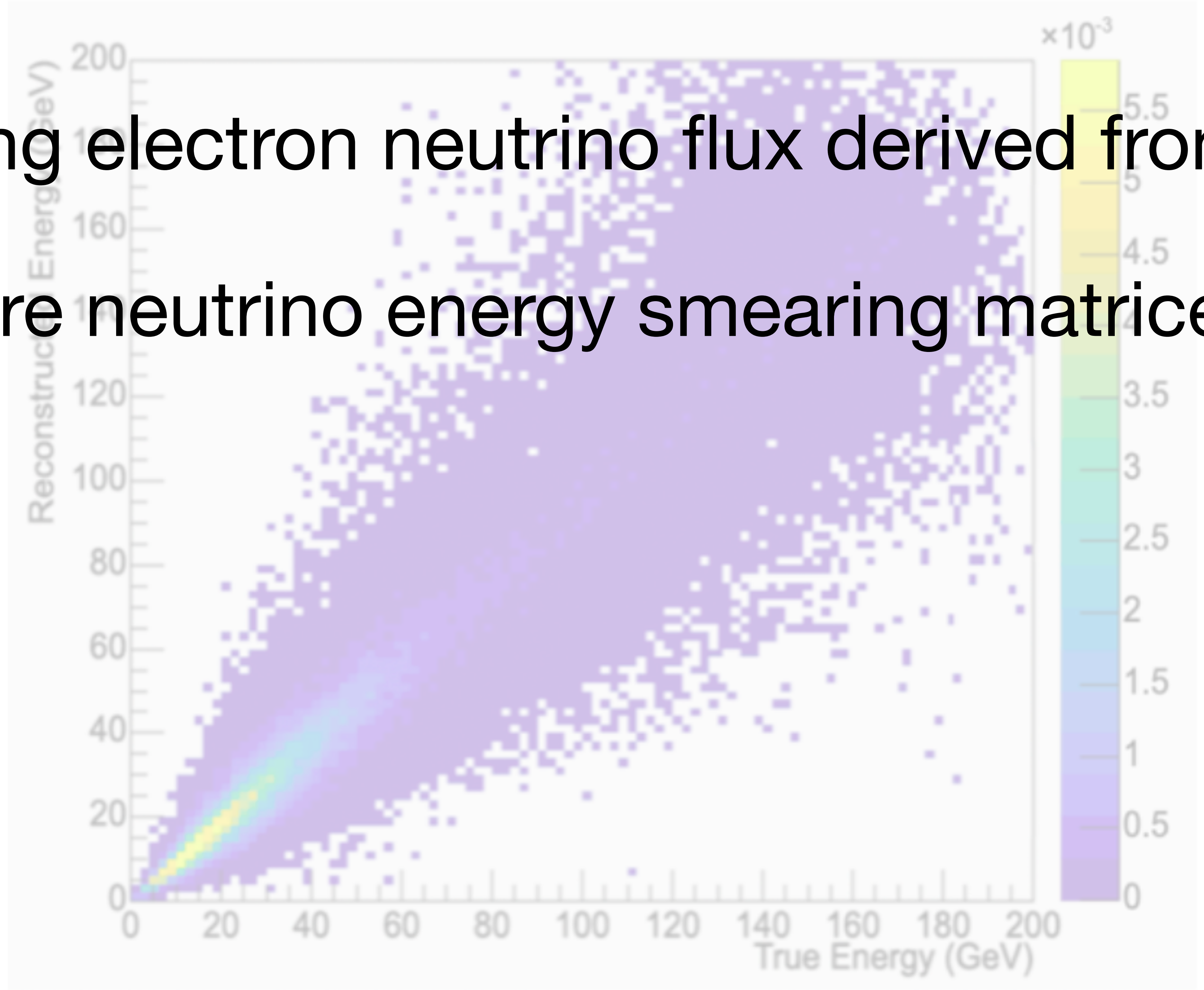

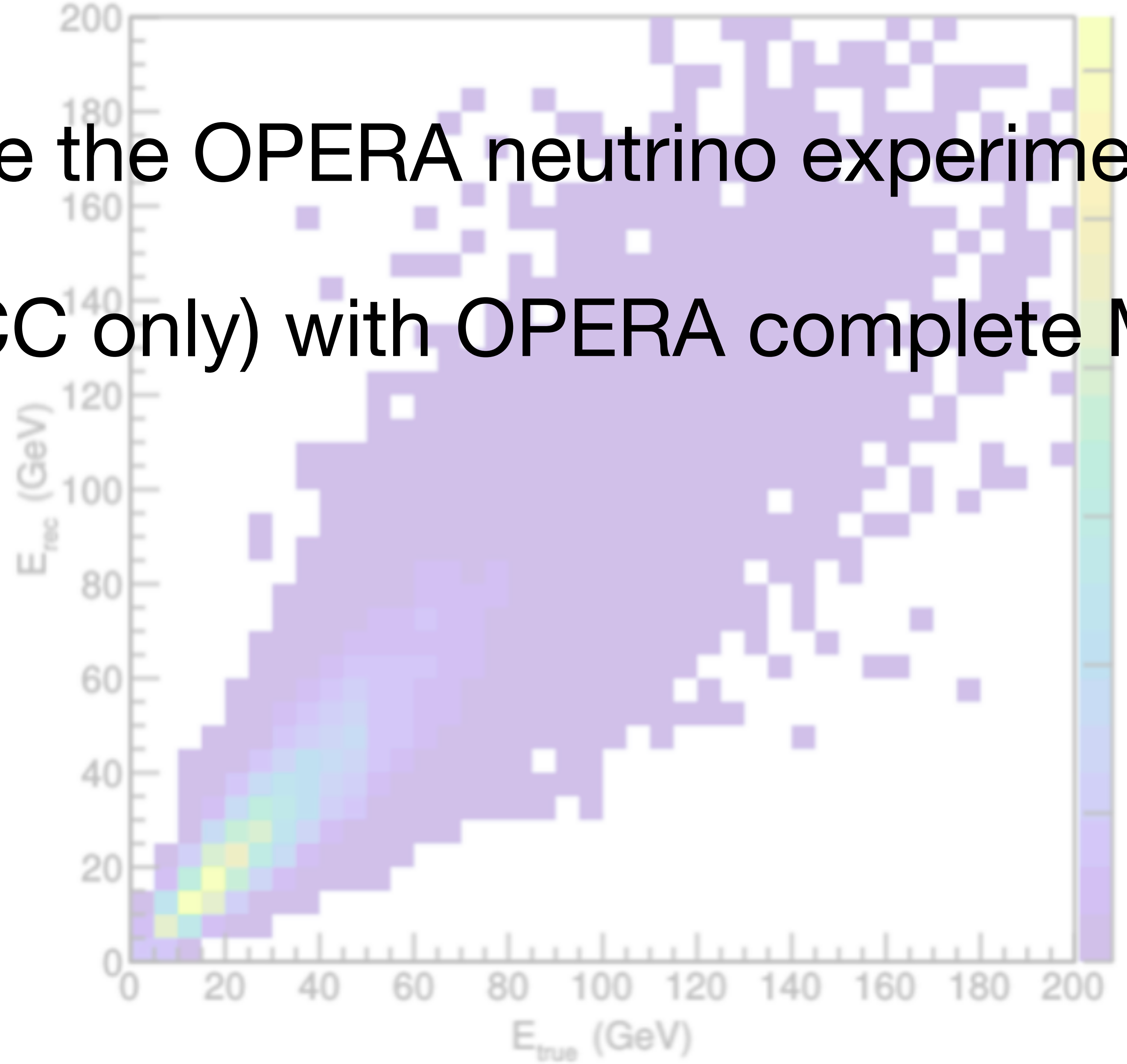

Energy Smearing - Complete MC Comparison

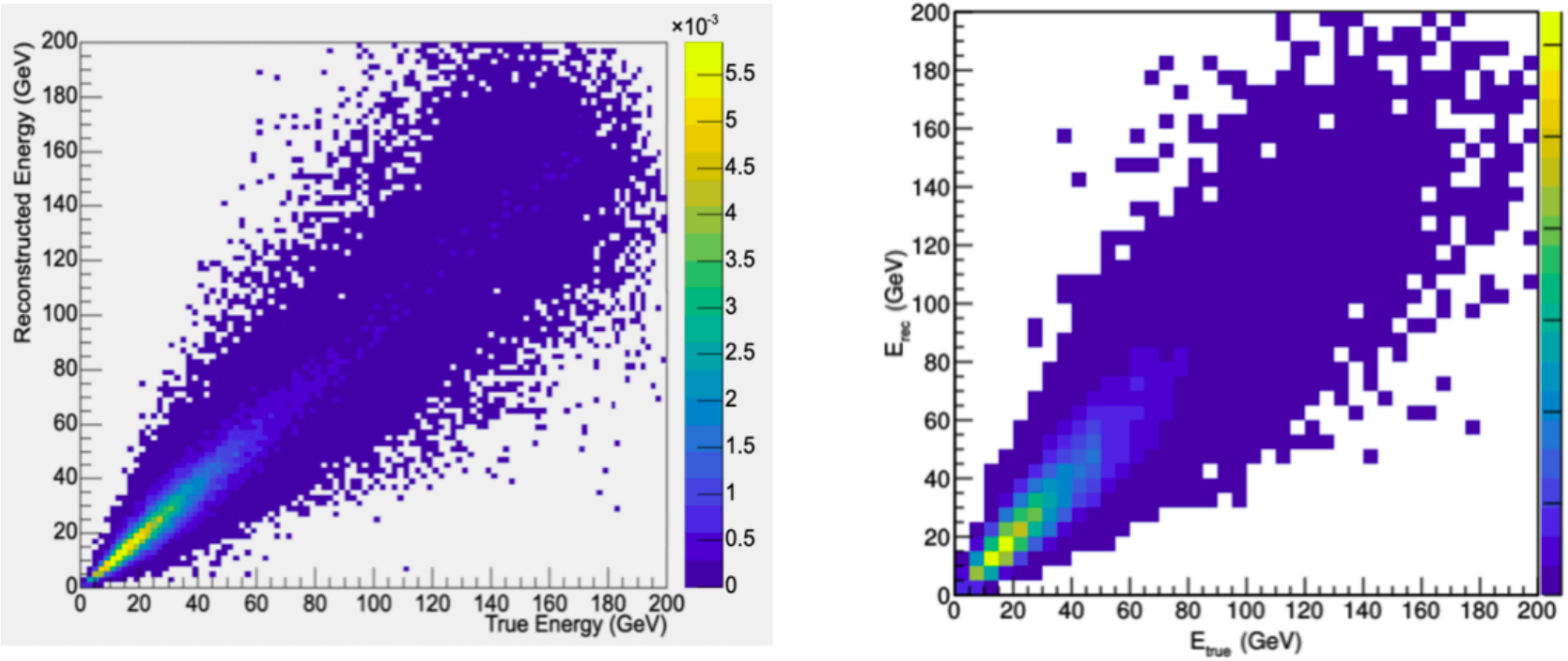

Figure 5: NuSmear Default (left) compared to complete Monte Carlo simulation (right) electron neutrino charged-current (CC) energy smearing matrices for the OPERA detector in the CNGS beam.

Energy Smearing - Deconstructed by Particle Type

DUNE-CDR Model

- Muon neutrinos incident on an Argon-40 target.
- Matrices deconstructed into multiple smearing matrices according to final state particle type.
- Agreement with the resolution functions and detection dependencies of the model:
    - Electrons, and positrons → less smearing.
    - Protons → more smearing.
    - Neutrons and antineutrons: energy reduced by constant factor (60% reconstruction).

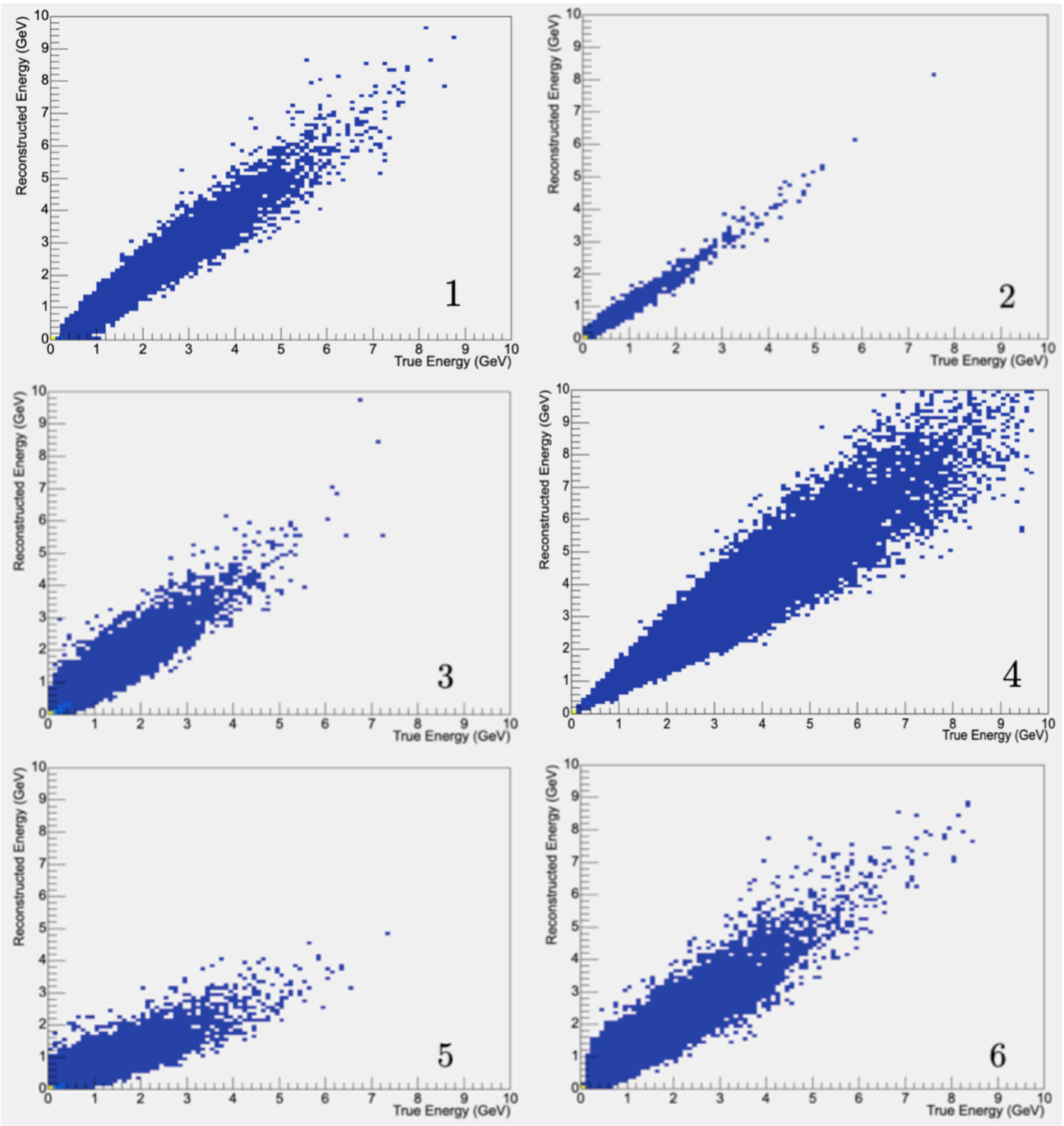

Figure 6: NuSmear DUNE-CDR energy smearing matrices deconstructed by final state particle type for muon neutrinos on an Argon-40 target - $\pi^{\pm}$ (1); γ, $e^{\pm}$ (2); $p/\bar{p}$ (3); $\mu^{\pm}$ (4); $n/\bar{n}$ (5); other (6).

Energy Smearing - Deconstructed by Particle Type

Default Model

- Again, agreement with the resolution functions and detection dependencies of the model:
  - Pions, muons, and kaons → less smearing
  - Protons/antiprotons and neutrons/antineutrons → more smearing.
  - Some data points in neutron/antineutron and photon matrices lie along the x-axis (50% detection dependency).

Particle type	Energy resolution
$\pi^{\pm}$,π^0	15%
$K^{\pm}$, $K^0/\bar{K}^0$	20%
γ	30%
$e^{\pm}$	40%
$p/\bar{p}$	40%
$\mu^{\pm}$	15%
$n/\bar{n}$	50%
other	30%

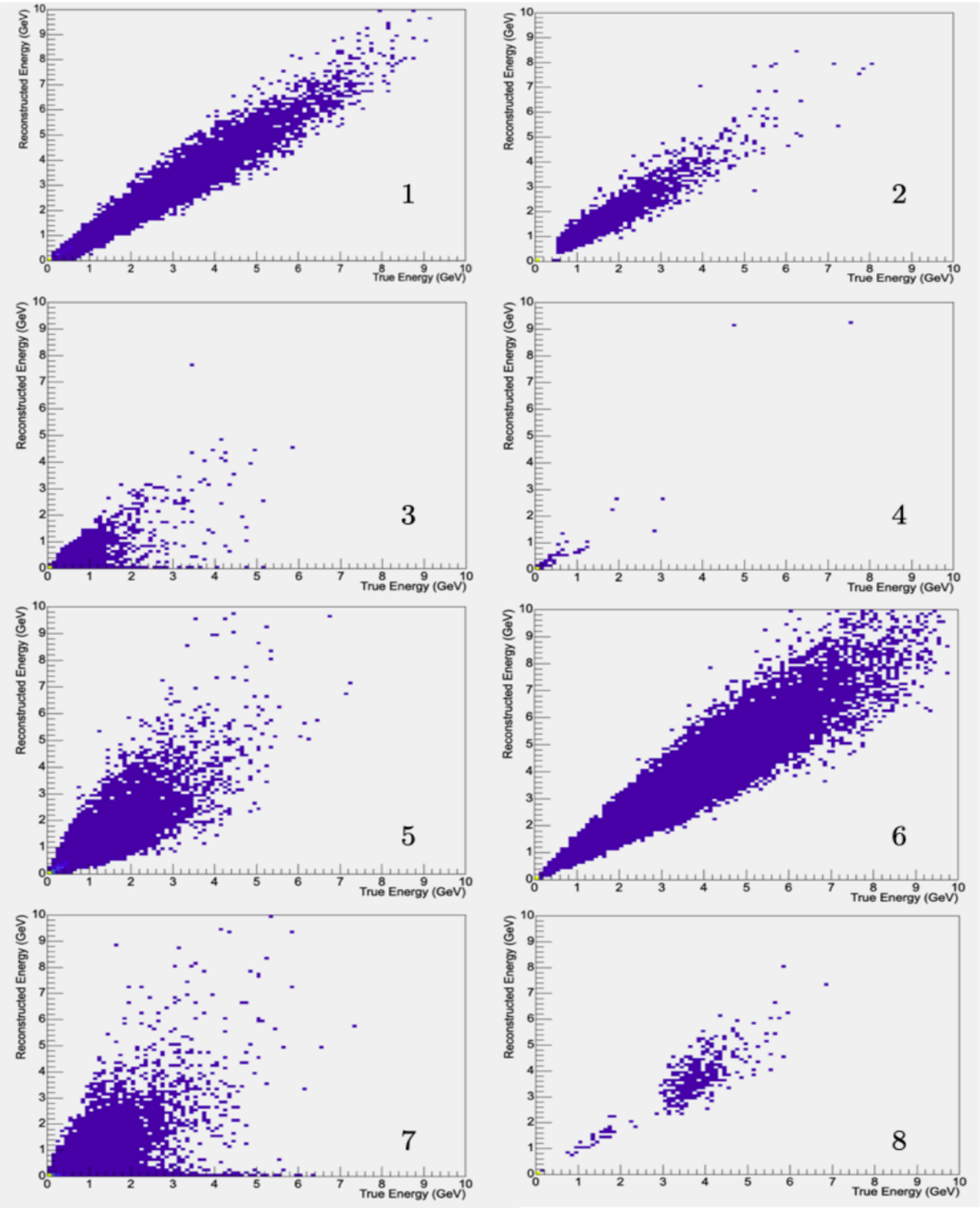

Figure 7: NuSmear Default energy smearing matrices deconstructed by final state particle type for muon neutrinos on an Argon-40 target - $\pi^{\pm}$,π^0 (1); $K^{\pm}$, $K^0/\bar{K}^0$ (2); γ (3); $e^{\pm}$ (4); $p/\bar{p}$ (5); $\mu^{\pm}$ (6); $n/\bar{n}$ (7); other (8).

Angular Smearing - Complete MC Comparison

- T2K Electron neutrino flux
- Electron angular smearing matrices for ND280 near detector (CC only).
- Agreement:
    - Main distribution.
    - Points spread further: complex effects beyond NuSmear's scope.

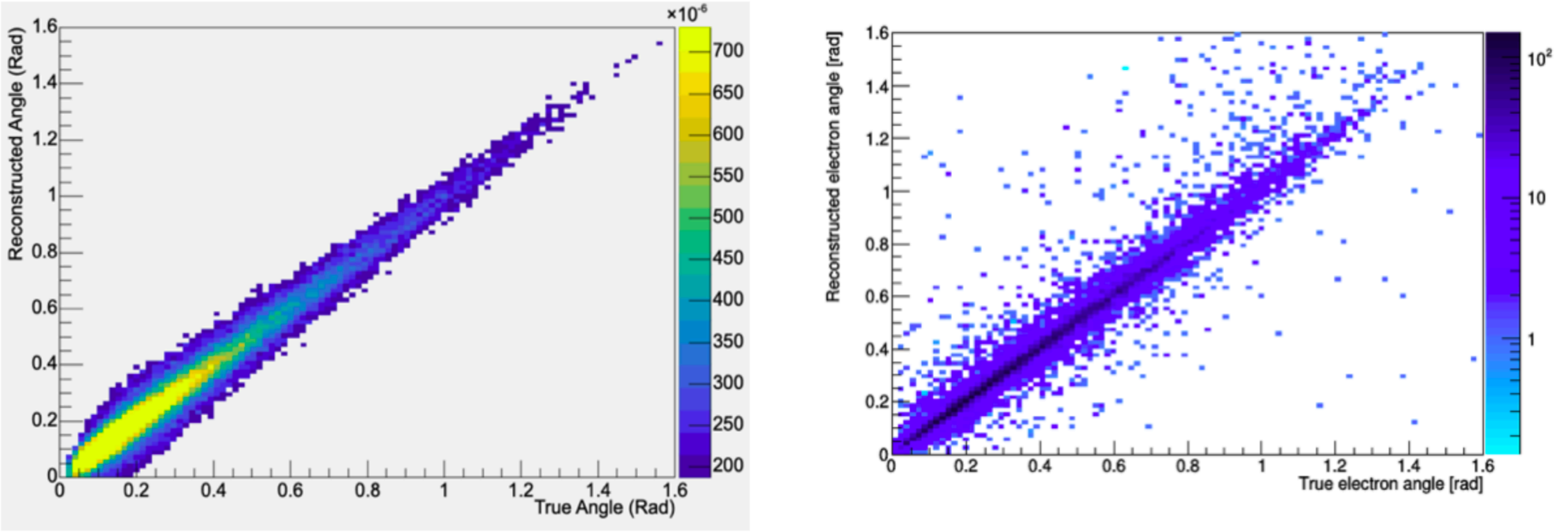

Figure 8: NuSmear Default model (left) compared to complete Monte Carlo simulation (right) electron angular smearing matrices for electron neutrino CC interactions at the T2K experiment's ND280 detector.

Angular Smearing - Deconstructed by Particle Type

- Charged pion and muon matrices → less smearing.
- Proton and neutron matrices → more smearing.
- Default smearing matrices exhibit more smearing than corresponding DUNE-CDR smearing matrices (more conservative).

Particle type	Angular resolution	
	DUNE-CDR model	Default model
$\pi^{\pm}$	1°	2°
π^0	5°	8°
$K^{\pm}$	5°	2°
$K^0/\bar{K^0}$	5°	8°
γ, $e^{\pm}$	1°	3°
$p/\bar{p}$	5°	8°
$\mu^{\pm}$	1°	2°
$n/\bar{n}$	5°	10°
other	5°	8°

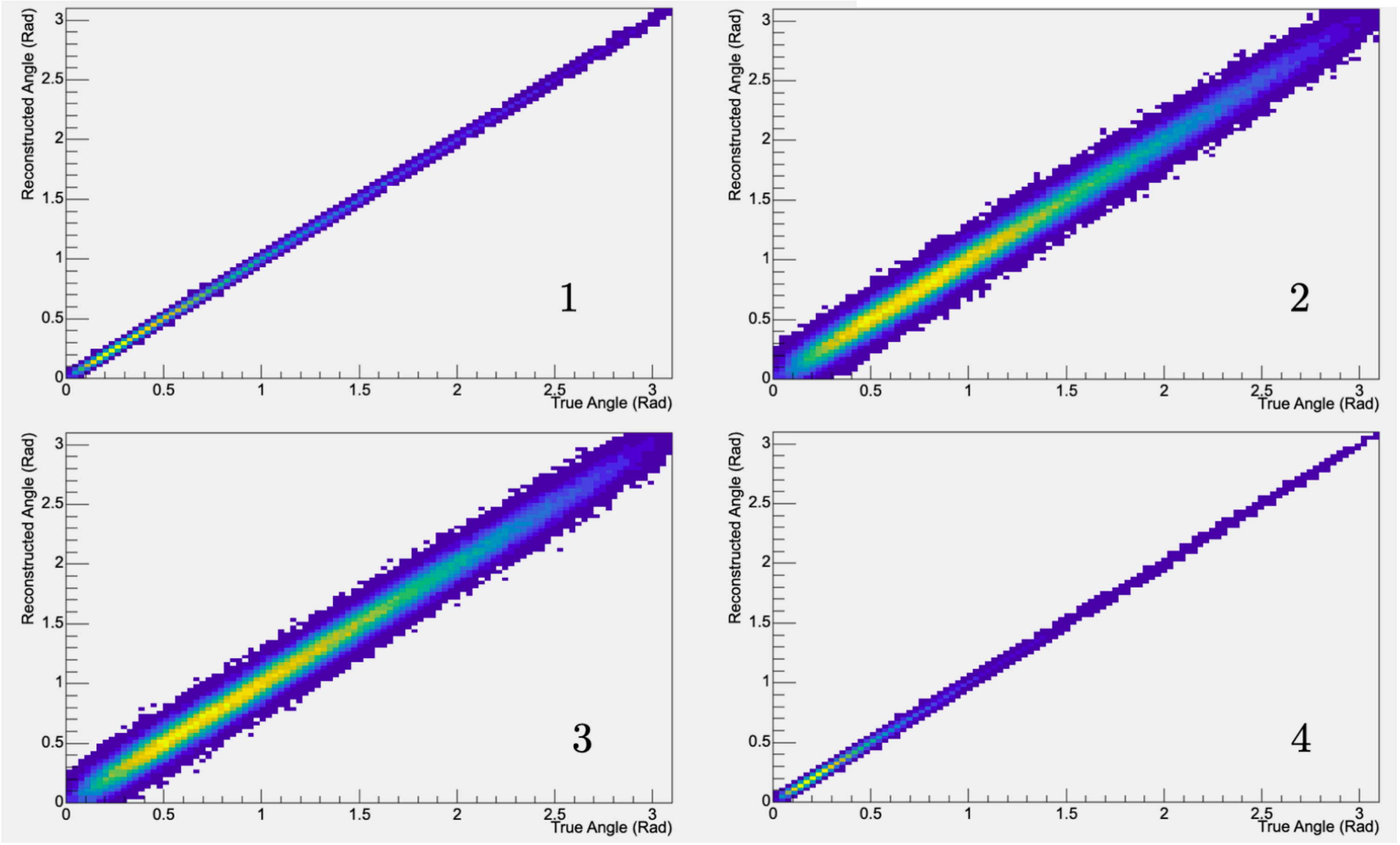

(a) DUNE-CDR angular smearing matrices

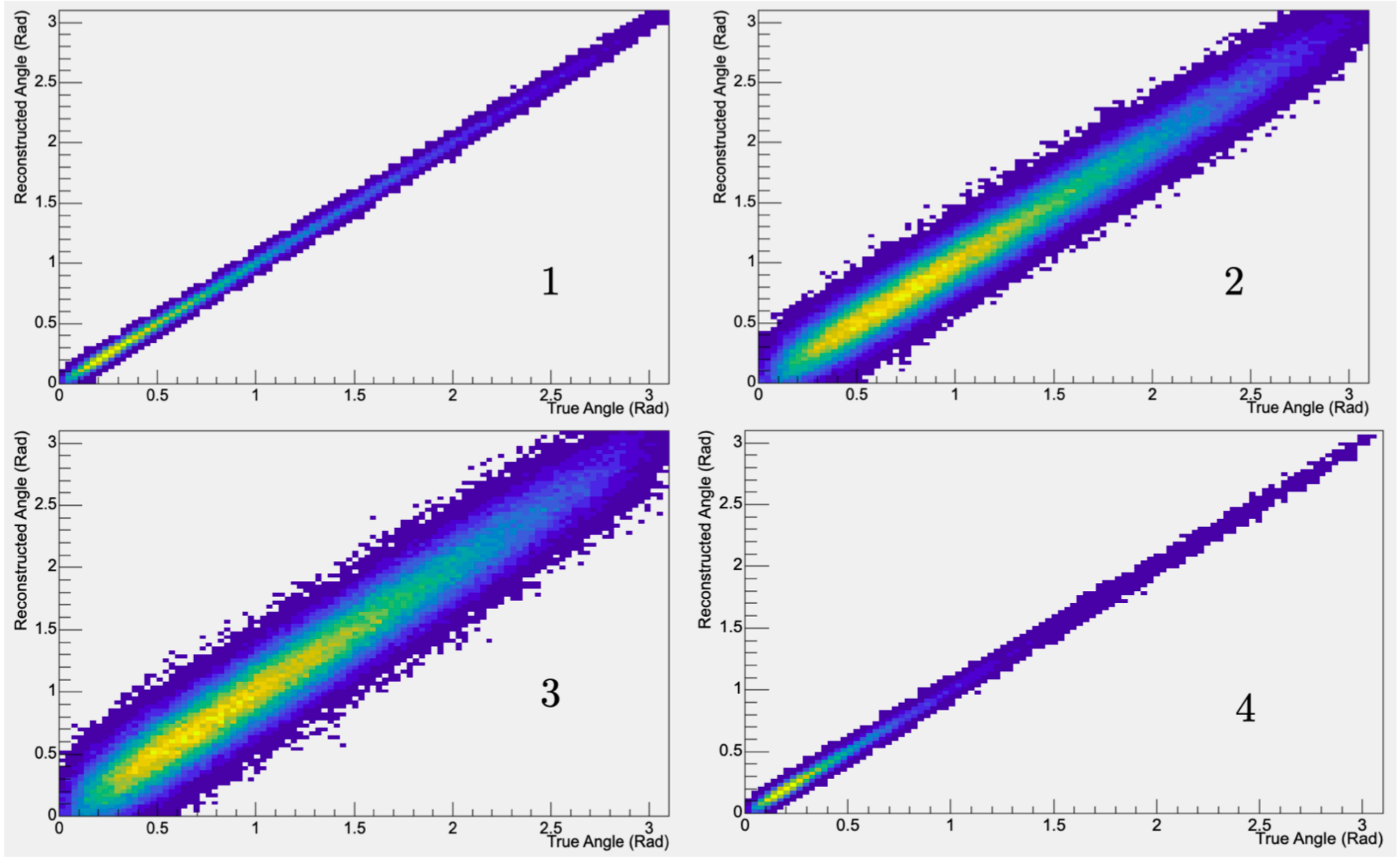

(b) Default angular smearing matrices

Figure 9: NuSmear DUNE-CDR and Default angular smearing matrices deconstructed by final state particle type for muon neutrinos on an Argon-40 target - $\pi^{\pm}$ (1); $p/\bar{p}$ (2); $n/\bar{n}$ (3); $\mu^{\pm}$ (4).

Summary

- Generic, fast, parameterized system for modeling energy smearing and angular smearing.
  - Model selection, resolution computation, application of distribution, detection dependency (for energy smearing only).

- Validation of NuSmear's performance
  - Strong adherence to the input models.
  - Accurate reproduction of independent complete Monte Carlo simulation.

Future Prospects

The future of NuSmear

- Open access, adjustable smearing models - NuSmear naturally lends itself to user customization.
- Ranges from tweaking values to implementing new smearing models - *potentially limitless complexity.*
- Greater control, more precise simulation capabilities over a wide range of parameters.

Acknowledgements

- This research project was undertaken as part of an internship at the University of Liverpool in the area of computational particle physics.
- I would like to sincerely thank my mentor, Dr. Marco Roda, for guiding me through this project and for offering helpful advice on my simulations and data analysis.
- I am also grateful to Professor Costas Andreopoulos for supervising my internship and providing me with the opportunity to conduct particle physics research as a high school student.
- Lastly, I would like to thank the Oliver Lodge Laboratory for hosting me and providing me with a comfortable environment to pursue my research.

References

1. M. H. Seymour and M. Marx, “Monte carlo event generators,” in LHC Phenomenology, pp. 287–319, Springer, 2015.
2. M. Tanabashi et al., “Particle data group,” Phys. Rev. D, vol. 98, no. 3, p. 030001, 2018.
3. C. Bozzi, “Monte carlo simulation in particle physics,” November 2002.
4. G. Iaselli, “A fast monte carlo event generator for particle physics,”
5. Nuclear Instruments and Methods in Physics Research Section A: Ac- celerators, Spectrometers, Detectors and Associated Equipment, vol. 248, no. 2, pp. 488–490, 1986.
6. J. Y. Araz, B. Fuks, and G. Polykratis, “Simplified fast detector simula- tion in madanalysis 5,” The European Physical Journal C, vol. 81, no. 4, pp. 1–24, 2021.
7. T. Wlodek, “Monte carlo methods in high energy physics,” June 2002. B. Siddi, “Development and deployment of a fast monte carlo simulation in lhcb,” Il nuovo cimento C, vol. 41, no. 1-2, pp. 1–2, 2018.
8. A. Accardi, J. Albacete, M. Anselmino, N. Armesto, E. Aschenauer,
9. A. Bacchetta, D. Boer, W. Brooks, T. Burton, N.-B. Chang, et al., “Electron-ion collider: The next qcd frontier,” The European Physical Journal A, vol. 52, no. 9, pp. 1–100, 2016.
10. C. Delaere, “” delphes: Framework for fast simulation of a generic collider experiment,” in MC4BSM 2013-Monte Carlo Tools for Physics Beyond the Standard Model, 2013.
11. L. Koch, “A response-matrix-centred approach to presenting cross-section measurements,” Journal of Instrumentation, vol. 14, no. 09, p. P09013, 2019.
12. A. Buckley, D. Kar, and K. Nordstr¨om, “Fast simulation of detector effects in rivet,” SciPost Physics, vol. 8, no. 2, p. 025, 2020.
13. S. Hamilton, K. Sliwa, S. Zimmermann, W. Lukas, J. Wetter, E. Ritsch, E. Kneringer, S. Todorova, and A. Salzburger, “The atlas fast track simulation project,” tech. rep., ATL-COM-SOFT-2010-070, 2011.
14. P. Huber, M. Lindner, and W. Winter, “Simulation of long-baseline neutrino oscillation experiments with globes:(general long baseline exper- iment simulator),” Computer Physics Communications, vol. 167, no. 3, pp. 195–202, 2005.
15. C. Andreopoulos, A. Bell, D. Bhattacharya, F. Cavanna, J. Dobson, S. Dytman, H. Gallagher, P. Guzowski, R. Hatcher, P. Kehayias, et al.,
16. “The genie neutrino monte carlo generator,” Nuclear Instruments and Methods in Physics Research Section A: Accelerators, Spectrometers, Detectors and Associated Equipment, vol. 614, no. 1, pp. 87–104, 2010.
17. R. Acciarri, M. Acero, M. Adamowski, C. Adams, P. Adamson, S. Ad- hikari, Z. Ahmad, C. Albright, T. Alion, E. Amador, et al., “Long-baseline neutrino facility (lbnf) and deep underground neutrino experiment (dune) conceptual design report, volume 4 the dune detectors at lbnf,” arXiv preprint arXiv:1601.02984, 2016.
18. B. Abi, R. Acciarri, M. A. Acero, G. Adamov, D. Adams, M. Adinolfi, Z. Ahmad, J. Ahmed, T. Alion, S. A. Monsalve, et al., “Deep underground neutrino experiment (dune), far detector technical design report, volume ii: Dune physics,” arXiv preprint arXiv:2002.03005, 2020.
19. T. Alion, J. Back, A. Bashyal, M. Bass, M. Bishai, D. Cherdack, M. Diwan, Z. Djurcic, J. Evans, E. Fernandez-Martinez, et al., “Ex- periment simulation configurations used in dune cdr,” arXiv preprint arXiv:1606.09550, 2016.
20. L. Lyons, “Statistical issues in particle physics,” in Particle Physics Reference Library, pp. 645–692, Springer, 2020.
21. M. Matsumoto and T. Nishimura, “Mersenne twister: a 623-dimensionally equidistributed uniform pseudo-random number generator,” ACM Trans- actions on Modeling and Computer Simulation (TOMACS), vol. 8, no. 1, pp. 3–30, 1998.
22. N. Agafonova, A. Aleksandrov, A. Anokhina, S. Aoki, A. Ariga, T. Ariga, A. Bertolin, C. Bozza, R. Brugnera, A. Buonaura, et al., “Final results of the search for $\nu_\mu \rightarrow \nu_e$ oscillations with the opera detector in the cngs beam,” Journal of High Energy Physics, vol. 2018, no. 6, pp. 1–15, 2018.
23. K. Abe, N. Akhlaq, R. Akutsu, A. Ali, C. Alt, C. Andreopoulos, L. An- thony, M. Antonova, S. Aoki, A. Ariga, et al., “Measurement of the charged-current electron (anti-) neutrino inclusive cross-sections at the t2k off-axis near detector nd280,” Journal of High Energy Physics, vol. 2020, no. 10, pp. 1–43, 2020.
24. E. Aschenauer, T. Burton, R. Darienzo, and A. Kiselev, “Eic detector simulations,” 2013.

Further Angular Smearing Matrices - Deconstructed by Particle Type

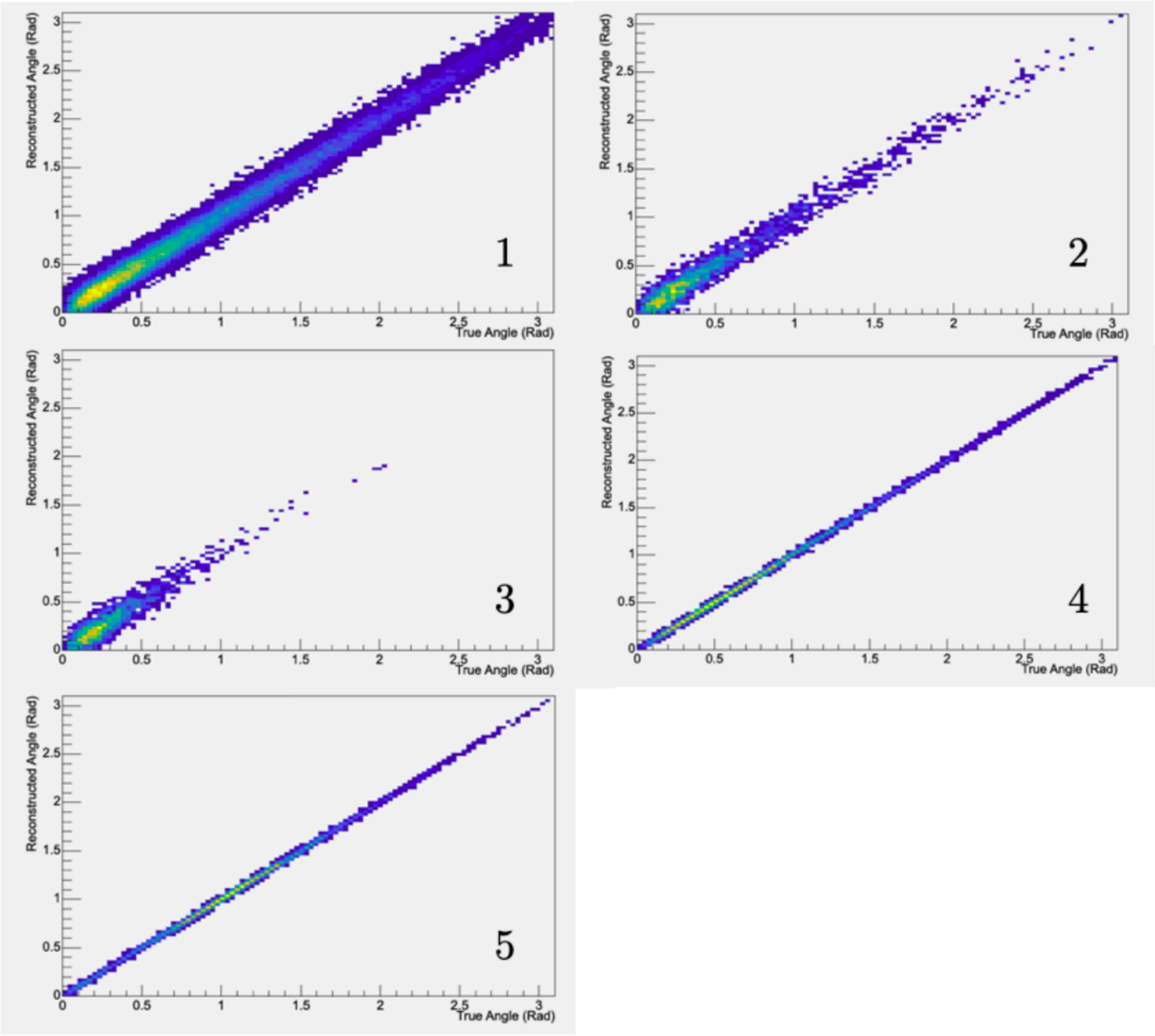

Figure 10: NuSmear DUNE-CDR angular smearing matrices deconstructed by final state particle type for muon neutrinos on an Argon-40 target - π^0 (1); $K^{\pm}$ (2); $K^0/\bar{K}^0$ (3); γ, $e^{\pm}$ (4); other (5).

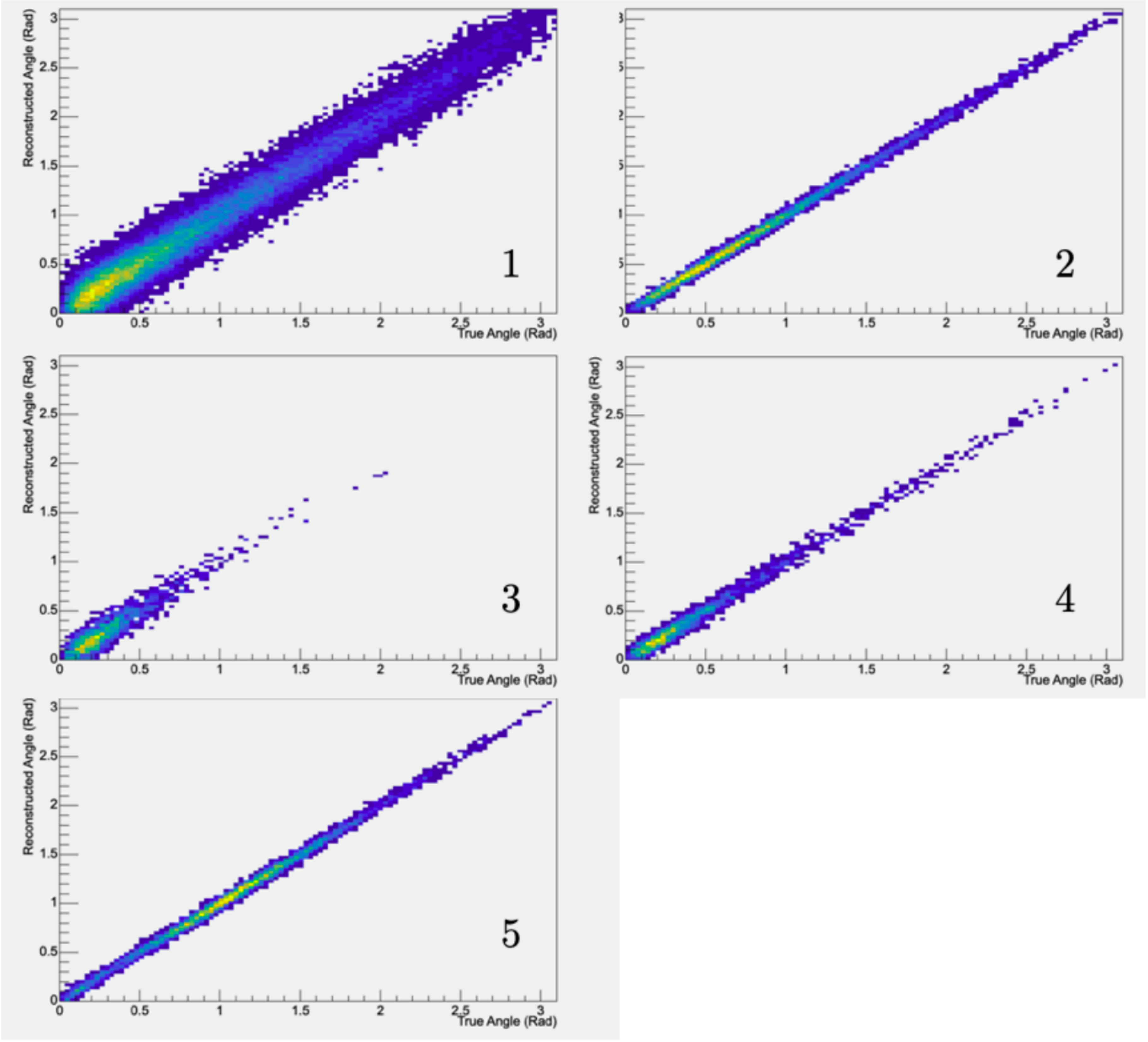

Figure 11: NuSmear Default angular smearing matrices deconstructed by final state particle type for muon neutrinos on an Argon-40 target - π^0 (1); $K^{\pm}$ (2); $K^0/\bar{K}^0$ (3); γ, $e^{\pm}$ (4); other (5).